JACS
JOURNAL OF THE AMERICAN CHEMICAL SOCIETY
pubs.acs.org/JACS
Communication

Assessing the Photoinduced Electron-Donating Behavior of Carbon Nanodots in Nanoconjugates

Andrés Ferrer-Ruiz, Tobias Scharl, Laura Rodríguez-Pérez, Alejandro Cadranel, M. Ángeles Herranz,* Nazario Martín,* and Dirk M. Guldi*

Cite This: J. Am. Chem. Soc. 2020, 142, 20324−20328
Read Online
ACCESS | Metrics & More | Article Recommendations | Supporting Information

ABSTRACT: Carbon nanodots (CNDs) undergo electron transfer in different scenarios. Previous studies have mainly focused on the electron-accepting features of CNDs in covalently linked donor−acceptor nanoconjugates. In view of this, we decided to carry out in this study the formation of covalently linked nanoconjugates that feature electron-donating pressure synthesized carbon nanodots (**pCNDs**) and electron-accepting 11,11,12,12-tetracyano-9,10-anthra-*p*-quinodimethane (**TCAQ**): **pCND-TCAQ**. The stability of the one-electron reduced form of TCAQ renders it the acceptor of choice. Detailed structural and electrochemical investigations allowed the characterization of **pCND-TCAQ**. Furthermore, investigations regarding intramolecular interactions, by means of steady-state and pump−probe transient absorption spectroscopies, allowed detection and characterization of three excited state species, in general, and the **pCND$^{\bullet+}$-TCAQ$^{\bullet-}$** charge-separated state, in particular.

Carbon dots (CDs) have recently emerged as strongly photoluminiscent carbon materials.[1] The family of CDs comprises different types of quasi-spherical nanoparticles, with dimensions smaller than 20 nm. Commonly, they are categorized into different subgroups: graphene quantum dots (GQDs), carbon quantum dots (CQDs), carbon nanodots (CNDs), and polymer-like dots (PDs).[2−5] CNDs are amorphous nanoparticles, which are fabricated from easily affordable organic precursors, natural products, or waste, and which compared to inorganic nanoparticles exhibit a remarkable biocompatibility and eco-friendliness. These properties render CNDs relevant for applications in the areas of biology and medicine. Notable examples are cellular imaging, biosensors, or drug delivery.[6,7]

Depending on the molecular precursors, which were employed in the synthesis of CNDs, diverse functional groups are present on their surface. These constitute a unique platform for covalent as well as noncovalent chemistry to connect, for example, light harvesters, electron acceptors, or electron donors to them. An important feature of CNDs is their duality in charge transfer events acting either as electron donor or as electron acceptor.[8] In this regard, CNDs have been decorated with photo- and redox-active building blocks for energy and/or charge transfer processes, artificial photosynthesis, and, more recently, solar energy conversion devices.[9,10] Leading examples are the combination with SWCNTs,[11] polyoxometalates,[12] or transition metal dichalcogenides.[13]

CNDs have been covalently grafted with electron-donating π-extended tetrathiafulvalenes,[14] phthalocyanines,[15] and porphyrins.[16] In these nanoconjugates, a common feature is intramolecular electronic interactions between CNDs, on one hand, and electron donors or acceptors, on the other hand. As a matter of fact, an intramolecular charge separation follows light absorption. Charge-transfer events in covalent nanoconjugates of CNDs, in which they act as electron donors, remain elusive and largely unexplored to date. The only notable exception is a recent report on rylene diimides.[17]

Therefore, it is timely and imperative to make progress in the study of covalent conjugates of CNDs with electron acceptors. To this end, the electron-accepting 11,11,12,12-tetracyano-9,10-anthra-*p*-quinodimethane (**TCAQ**) was selected. Important is the enhanced stability of its one-electron reduced form, which results in a low reduction potential. **TCAQ** gains planarity and aromaticity upon reduction, spreading the charge over the two dicyanomethylenes and the central anthracene.[18]

For the preparation of the CNDs, we followed a multicomponent methodology using the widely employed citric acid and urea as starting materials, which were heated in a microwave reactor maintaining the pressure constant.[19] Pressure control limits the escape of gaseous byproducts from the solution, causing formation of pressure-induced CNDs (**pCND**) to terminate at an early stage.[20] Subsequently, the as-prepared **pCNDs** were treated with $SOCl_2$ at 70 °C to transform the carboxylic acids present on their surface in acyl chlorides. Afterward, the acyl chlorides reacted *in situ* with 2-hydroxymethyl-TCAQ[21] in an esterification reaction to afford the **pCND-TCAQ** hybrids (Scheme 1).

After isolation and purification (see Supporting Information for details), AFM measurements served to evaluate the morphology of the **pCND-TCAQ** nanoconjugates (Figure S1). Statistical analyses revealed the presence of particles with

Received: September 22, 2020
Published: November 19, 2020

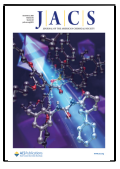

https://dx.doi.org/10.1021/jacs.0c10132
J. Am. Chem. Soc. 2020, 142, 20324−20328

Scheme 1. Synthesis of pCND-TCAQ Nanoconjugates

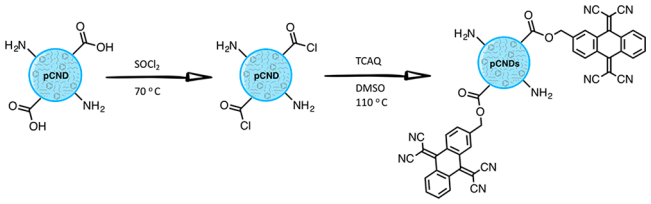

an average height of 4.3 ± 1.5 nm, which are somewhat larger than that observed for **pCNDs** (2.1 ± 1.1 nm).[14] The increase in size after the introduction of TCAQs might be due to $\pi-\pi$ interactions between TCAQs of different **pCND-TCAQ** nanoconjugates resulting in larger aggregates.[22]

The thermal stability of the obtained material was compared with that of the precursors, namely **pCND** and **TCAQ**. A similar weight loss is observed for both **pCND** and **pCND-TCAQ**, although a gradual and continuous weight loss was noted for the latter (Figure S2). Additional evidence for **pCND-TCAQ** nanoconjugation came from structural characterization by means of FTIR and XPS spectroscopies (Figures S3 and S4). On one hand, the FTIR spectrum of **pCND-TCAQ** revealed the presence of the stretching vibration of the cyano groups at 2208 cm^{-1} and the C═O vibration due to ester groups at 1735 cm^{-1} (Figure 1). On the other hand, the XPS high-resolution N 1s core-level spectrum of **pCND-TCAQ** was composed of five components as depicted in Figure 1. Four of these components were previously observed in the starting material and correspond to graphitic-N, pyrrolic-N, $-NH_2$, and pyridinic-N,[14] whereas the new component at 398.1 eV corresponds to the cyano groups of the TCAQs. Comparison of the stretching vibration (FTIR) and binding energy (XPS) of the cyano groups with reference systems allows concluding the presence of some charge-transfer in the **pCND-TCAQ** nanoconjugates.[23,24]

The steady-state absorption and fluorescence spectra of **pCND**, **TCAQ**, and **pCND-TCAQ** were measured in methanol at room temperature (Figure 2). The absorption spectrum of **pCND** displays a maximum at 365 nm and a tail that extends into the visible part of the solar spectrum, while a maximum at 340 nm is discernible for **TCAQ**. Importantly, the absorption features of **pCND-TCAQ** differ from a simple superposition of those from its constituents. For **pCND-TCAQ**, a maximum at 328 nm and a shoulder at 397 nm are detected. This points to strong electronic interactions between pCND and TCAQ in **pCND-TCAQ** in the ground state. Importantly, mixtures of **pCND** and **TCAQ** at 1:1, 1:5, and 5:1 ratios failed to exhibit the absorption features of **pCND-TCAQ**. They reveal a single absorption, which red-shifts slightly as a function of **pCND** (Figure S5). At this point we conclude only weak electronic interactions.

Also indicative for the electronic interactions are electrochemical measurements (Figure 3). Reduction of **TCAQ** is observed at −0.30 V vs Ag/AgCl in methanol, while the same reduction shifts in **pCND-TCAQ** to −0.62 V. Implicit are ground-state charge-transfer interactions, which shift electron density from pCND to TCAQ and render TCAQ more difficult to reduce in **pCND-TCAQ** than in **TCAQ**. Next, we probed mixtures of **pCND** and **TCAQ** by means of electrochemical measurements. Notable is the fact that the TCAQ reduction shifts upon addition of **pCNDs**, but only marginally within a range of 0.1 V (Figure S6). In line with the absorption measurements, we infer the presence of electronic interactions in these mixtures, but much weaker than those observed in **pCND-TCAQ**.

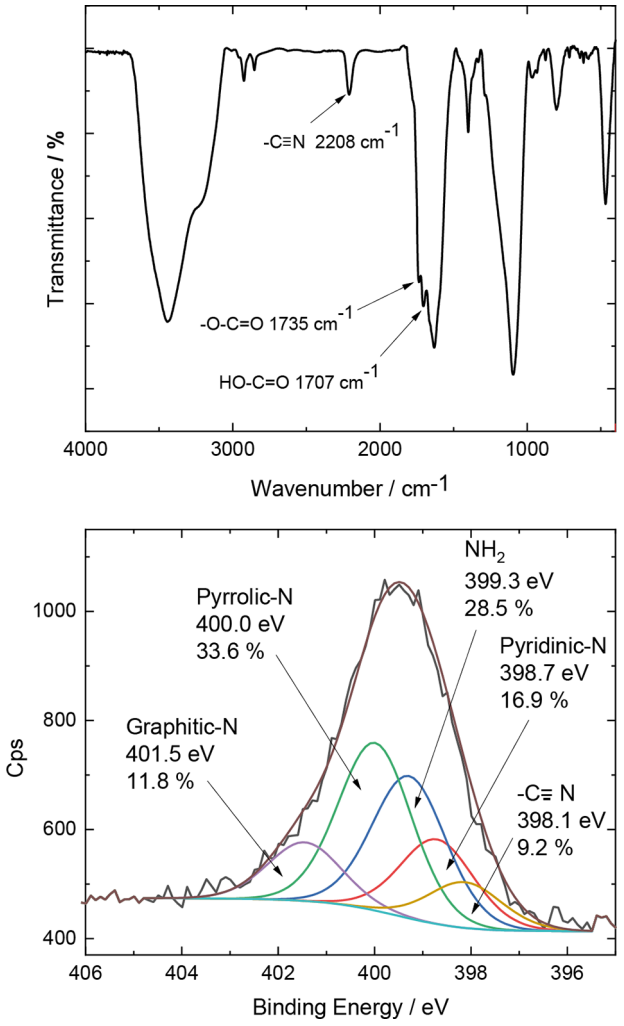

Figure 1. Top: FTIR spectrum of **pCND-TCAQ**. Bottom: XPS N 1s component deconvolution spectrum of **pCND-TCAQ**.

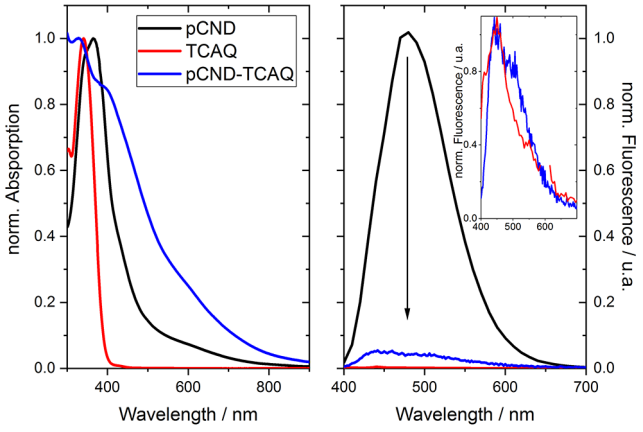

Figure 2. Left: Absorption spectra of **pCND**, **TCAQ**, and **pCND-TCAQ** recorded in methanol at room temperature. Right: fluorescence spectra of **pCND**, **TCAQ**, and **pCND-TCAQ** recorded with 343 nm photoexcitation in methanol at room temperature. Inset: normalized **TCAQ** and **pCND-TCAQ** fluorescence.

https://dx.doi.org/10.1021/jacs.0c10132
J. Am. Chem. Soc. 2020, 142, 20324−20328

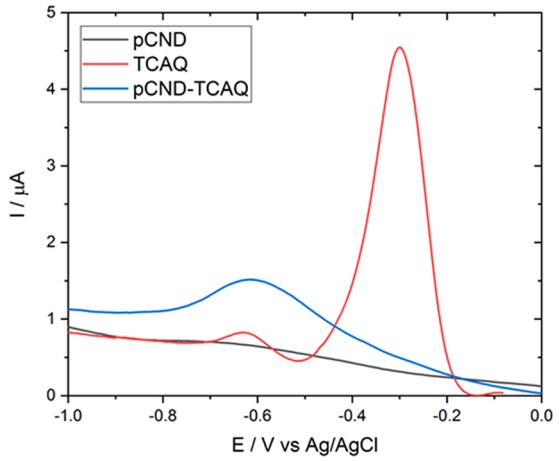

Figure 3. Square-wave voltammograms of **pCND**, **TCAQ**, and **pCND-TCAQ** nanoconjugate recorded in methanol at room temperature.

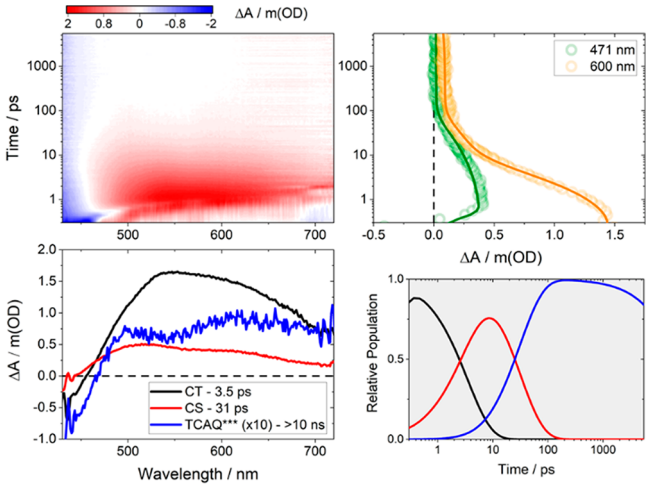

Figure 4. Top left: Differential absorption 3D map obtained upon fsTAS on **pCND-TCAQ** in methanol at room temperature, with 387 nm photoexcitation. Top right: Time absorption profiles and corresponding fittings at 471 (green) and 600 (orange) nm. Bottom left: Species associated differential spectra of $pCND^{\delta+}$-$TCAQ^{\delta-}$ (CT; black), $pCND^{\bullet+}$-$TCAQ^{\bullet-}$ (CS, red), and TCAQ*** (blue) excited states. Bottom right: concentration evolution over time.

Moreover, electronic interactions were analyzed in the excited state by illuminating the samples at 343 nm (Figure 2). **pCND** emits light at 470 nm in methanol at room temperature, with a quantum yield of 18%. **TCAQ** features a weak fluorescence at 450 nm with a quantum yield of <0.01%. In **pCND-TCAQ**, the pCND-centered fluorescence is strongly quenched, and a quantum yield of only 1% is observed. From the quenching we conclude strong intramolecular electronic interactions in their excited state, which open energy or electron transfer quenching pathways. The fluorescence spectrum of **pCND-TCAQ** resembles that of **TCAQ**, which is consistent with transient studies (*vide infra*).

To shed light on the excited state dynamics, which are connected to the steady-state observations, femtosecond transient absorption spectroscopy (fsTAS) was performed. We used 387 nm excitation and methanol as solvent at room temperature. **TCAQ** initially shows strong photoinduced absorptions, which display 480 and 550 nm shoulders upon laser excitation (Figure S7). All of the aforementioned absorption features decay, however, rapidly and within 10 ps, only very weak photoinduced absorptions are observed. These are persistent on the nanosecond time scale, a behavior which is consistent with the weak emission observed in the steady-state experiments. Global analyses of the data were based on a three-species kinetic model. The corresponding three lifetimes are 0.7 ps, 43 ps, and >10 ns, and their evolution-associated spectra are depicted in Figure S3. These spectra are ascribed to three sequentially populated excited states: TCAQ*, TCAQ**, and TCAQ***. TCAQ* is the excited state populated upon light absorption and displays intense and broad photoinduced absorptions all throughout the visible range, where shoulders at 480 and 575 nm can be discerned. In 700 fs, it feeds TCAQ**. This state gives rise to much weaker photoinduced absorptions at 450 and 600 nm, and feeds TCAQ*** in 43 ps. Noteworthy, TCAQ*** is responsible for the weak fluorescence detected in the steady-state experiments. Its differential spectrum is characterized by a broad positive signal that maximizes at 600 nm and shoulders at around 500 nm. **pCNDs** were previously studied under these conditions. From negative signals in the 470−700 nm region, we concluded time constants of 6.1, 71.9, and 7000 ps.[25]

The behavior of **pCND-TCAQ** upon laser excitation is completely different from that of its constituents (Figure 4). Initially, a broad positive photoinduced absorption with a 550 nm maximum is observed, together with a negative signal at wavelengths shorter than 450 nm. Within about 150 ps, only signals remain, which are 10 times weaker than those at shorter time scales. For global analyses of the data we developed a three-species kinetic model, which led to lifetimes of 3.5 ps, 31 ps, and >10 ns. The resulting evolution-associated spectra are displayed in Figure 4. As the first species, a charge-transfer state with a $\mathbf{pCND^{\delta+}}$-$\mathbf{TCAQ^{\delta-}}$ electronic configuration is instantly populated with light absorption (CT, black curve in Figure 4). Then, as second species, the $\mathbf{pCND^{\bullet+}}$-$\mathbf{TCAQ^{\bullet-}}$ charge-separated state (CS, red curve in Figure 4) evolves from a charge separation, which takes place in 3.5 ps. Importantly, the differential spectra of the corresponding maxima in the region 520−600 nm resemble those observed upon spectroelectrochemical reduction of **TCAQ** at 540 nm in DMSO (Figure S8) or DMF[26] and reductive pulse radiolysis (maximum at 600 nm in toluene/isopropanol/acetone).[27] Charge recombination occurs in 31 ps and reinstates the ground state. The third species is the longest-lived component (TCAQ***, blue curve in Figure 4) and has a differential spectrum shape—albeit weak in intensity—that resembles that found for the TCAQ*** excited state in **TCAQ**. Features include maxima at around 500 and 600 nm. This excited state is responsible for the weak emission observed in the steady-state experiments. The absence of any charge separation was corroborated in blank experiments, which were performed with mixtures of **pCND** and **TCAQ** in either a 1:5 or a 5:1 ratio (Figures S9 and S10). Regardless of the relative ratio, both showed four species, with time constants of around 1−2 ps, 10−13 ps, 3.8 ns, and >10 ns. Their differential spectra display features ascribed to TCAQ*, pCND*, pCND**, and pCND***, respectively (Figures S9 and S10).

In conclusion, we have successfully prepared a covalently linked electron donor−acceptor nanoconjugate featuring **pCNDs** as electron donors and **TCAQs** as electron acceptors. **pCND-TCAQ** has been morphologically (AFM) and structurally (FTIR, XPS) characterized. Intramolecular electronic

https://dx.doi.org/10.1021/jacs.0c10132
J. Am. Chem. Soc. 2020, 142, 20324−20328

interactions were determined by electrochemical and photophysical means, in both the ground and excited states. Notably, charge separation evolves upon photoexcitation leading to a 31 ps lived charge-separated state. Our results underline that the covalent linkage between **pCND** and **TCAQ** is key to promote strong electronic interactions, in both the ground and electronically excited states, and to enable charge separation. Our work shows a remarkably structure−property relationship in newly engineered **pCND** conjugates and validates the versatility of **pCND**s as outstanding building blocks with amphoteric redox behavior. Their tunable chemical functionalization and electronic properties render them materials of choice for emergent nanotechnologies.

■ ASSOCIATED CONTENT

Supporting Information

The Supporting Information is available free of charge at https://pubs.acs.org/doi/10.1021/jacs.0c10132.

Materials and instrumental techniques details, synthetic procedures, and additional figures (PDF)

■ AUTHOR INFORMATION

Corresponding Authors

M. Ángeles Herranz − *Department of Organic Chemistry, Faculty of Chemistry, Complutense University of Madrid, Avda. Complutense s/n, Ciudad Universitaria, E-28040 Madrid, Spain;* orcid.org/0000-0001-9155-134X; Email: maherran@ucm.es

Nazario Martín − *Department of Organic Chemistry, Faculty of Chemistry, Complutense University of Madrid, Avda. Complutense s/n, Ciudad Universitaria, E-28040 Madrid, Spain; IMDEA-Nanociencia, 28049 Madrid, Spain;* orcid.org/0000-0002-5355-1477; Email: nazmar@ucm.es

Dirk M. Guldi − *Department of Chemistry and Pharmacy, Interdisciplinary Center for Molecular Materials, Friedrich-Alexander Universität Erlangen-Nürnberg, 91058 Erlangen, Germany;* orcid.org/0000-0002-3960-1765; Email: dirk.guldi@fau.de

Authors

Andrés Ferrer-Ruiz − *Department of Organic Chemistry, Faculty of Chemistry, Complutense University of Madrid, Avda. Complutense s/n, Ciudad Universitaria, E-28040 Madrid, Spain*

Tobias Scharl − *Department of Chemistry and Pharmacy, Interdisciplinary Center for Molecular Materials, Friedrich-Alexander Universität Erlangen-Nürnberg, 91058 Erlangen, Germany*

Laura Rodríguez-Pérez − *Department of Organic Chemistry, Faculty of Chemistry, Complutense University of Madrid, Avda. Complutense s/n, Ciudad Universitaria, E-28040 Madrid, Spain*

Alejandro Cadranel − *Department of Chemistry and Pharmacy, Interdisciplinary Center for Molecular Materials, Friedrich-Alexander Universität Erlangen-Nürnberg, 91058 Erlangen, Germany; Universidad de Buenos Aires, Facultad de Ciencias Exactas y Naturales, Departamento de Química Inorgánica, Analítica y Química Física, C1428EHA Buenos Aires, Argentina; CONICET − Universidad de Buenos Aires. Instituto de Química Física de Materiales, Medio Ambiente y Energía (INQUIMAE), Pabellón 2, Ciudad Universitaria, C1428EHA Buenos Aires, Argentina;* orcid.org/0000-0002-6597-4397

Complete contact information is available at: https://pubs.acs.org/10.1021/jacs.0c10132

Notes

The authors declare no competing financial interest.

■ ACKNOWLEDGMENTS

The authors thank the Spanish Ministry of Science, Innovation and Universities MCIU (Projects CTQ2017-84327-P and CTQ2017-83531-R). Additional support is acknowledged from the Deutsche Forschungsgemeinschaft (DFG) via SFB 953 "Synthetic Carbon Allotropes" and the Excellence Cluster "Engineering of Advanced Materials". AC thanks ALN for support. This paper is dedicated to Professor Andreas Hirsch on occasion of his 60th birthday.

■ REFERENCES

(1) Yao, B.; Huang, H.; Liu, Y.; Kang, Z. Carbon Dots: A Small Conundrum. *Trends Chem.* **2019**, *1*, 235−246.

(2) Cayuela, A.; Soriano, M. L.; Carrillo-Carrión, C.; Valcárcel, M. Semiconductor and carbon-based fluorescent nanodots: the need for consistency. *Chem. Commun.* **2016**, *52*, 1311−1326.

(3) Sekiya, R.; Uemura, Y.; Murakami, H.; Haino, T. White-Light-Emitting Edge-Functionalized Graphene Quantum Dots. *Angew. Chem., Int. Ed.* **2014**, *53*, 5619−5623.

(4) Li, R.; Liu, Y.; Li, Z.; Shen, J.; Yang, Y.; Cui, X.; Yang, G. Bottom-Up Fabrication of Single-Layered Nitrogen-Doped Graphene Quantum Dots through Intermolecular Carbonization Arrayed in 2D Plane. *Chem. - Eur. J.* **2016**, *22*, 272−278.

(5) Sekiya, R.; Haino, T. Chemically Functionalized Two-Dimensional Carbon Materials. *Chem. - Asian J.* **2020**, *15*, 2316−2328.

(6) Xiao, L.; Sun, H. Novel properties and applications of carbon nanodots. *Nanoscale Horiz.* **2018**, *3*, 565−597.

(7) Tian, X.-T.; Yin, X.-B. Carbon Dots, Unconventional Preparation Strategies, and Applications Beyond Photoluminescence. *Small* **2019**, *15*, 1901803.

(8) Srivastava, I.; Khamo, J. S.; Pandit, S.; Fathi, P.; Huang, X.; Cao, A.; Haasch, R. T.; Nie, S.; Zhang, K.; Pan, D. Influence of Electron Acceptor and Electron Donor on the Photophysical Properties of Carbon Dots: A Comparative Investigation at the Bulk-State and Single-Particle Level. *Adv. Funct. Mater.* **2019**, *29*, 1902466.

(9) Cadranel, A.; Margraf, J. T.; Strauss, V.; Clark, T.; Guldi, D. M. Carbon Nanodots for Charge-Transfer Processes. *Acc. Chem. Res.* **2019**, *52*, 955−963.

(10) Hu, C.; Li, M.; Qiu, J.; Sun, Y.-P. Design and fabrication of carbon dots for energy conversion and storage. *Chem. Soc. Rev.* **2019**, *48*, 2315−2337.

(11) Strauss, V.; Margraf, J. T.; Clark, T.; Guldi, D. M. A carbon-carbon hybrid - immobilizing carbon nanodots onto carbon nanotubes. *Chem. Sci.* **2015**, *6*, 6878−6885.

(12) Madonia, A.; Martin-Sabi, M.; Sciortino, A.; Agnello, S.; Cannas, M.; Ammar, S.; Messina, F.; Schaming, D. Highly Efficient Electron Transfer in a Carbon Dot-Polyoxometalate Nanohybrid. *J. Phys. Chem. Lett.* **2020**, *11*, 4379−4384.

(13) Vallan, L.; Canton-Vitoria, R.; Gobeze, H. B.; Jang, Y.; Arenal, R.; Benito, A. M.; Maser, W. K.; D'Souza, F.; Tagmatarchis, N. Interfacing transition metal dichalcogenides with carbon nanodots for managing photoinduced energy and charge-transfer processes. *J. Am. Chem. Soc.* **2018**, *140*, 13488−13496.

(14) Ferrer-Ruiz, A.; Scharl, T.; Haines, P.; Rodríguez-Pérez, L.; Cadranel, A.; Herranz, M. A.; Guldi, D. M.; Martín, N. Exploring Tetrathiafulvalene-Carbon Nanodot Conjugates in Charge Transfer Reactions. *Angew. Chem., Int. Ed.* **2018**, *57*, 1001−1005.

(15) Prato, M.; Cacioppo, M.; Scharl, T.; Đorđević, L.; Cadranel, A.; Arcudi, F.; Guldi, D. M. Symmetry-Breaking Charge Transfer

Chromophore Interactions Supported by Carbon Nanodots. *Angew. Chem., Int. Ed.* **2020**, *59*, 12779−12784.
(16) Arcudi, F.; Strauss, V.; Đorđević, L.; Cadranel, A.; Guldi, D. M.; Prato, M. Porphyrin Antennas on Carbon Nanodots: Excited State Energy and Electron Transduction. *Angew. Chem.* **2017**, *129*, 12265−12269.
(17) Đorđević, L.; Haines, P.; Cacioppo, M.; Arcudi, F.; Scharl, T.; Cadranel, A.; Guldi, D. M.; Prato, M. Synthesis and excited state processes of arrays containing amine-rich carbon dots and unsymmetrical rylene diimides. *Mater. Chem. Front.* **2020**, DOI: 10.1039/D0QM00407C.
(18) Ortí, E.; Viruela, R.; Viruela, P. M. Influence of Benzoannulation on the Molecular and Electronic Structures of Tetracyanoquinodimethanes. *J. Phys. Chem.* **1996**, *100*, 6138−6146.
(19) Strauss, V.; Kahnt, A.; Zolnhofer, E. M.; Meyer, K.; Maid, H.; Placht, C.; Bauer, W.; Nacken, T. J.; Peukert, W.; Etschel, S. H.; Halik, M.; Guldi, D. M. Assigning Electronic States in Carbon Nanodots. *Adv. Funct. Mater.* **2016**, *26*, 7975−7985.
(20) Hutton, G. A. M.; Martindale, B. C. M.; Reisner, E. Carbon dots photosensitisers for solar-driven catalysis. *Chem. Soc. Rev.* **2017**, *46*, 6111−6123.
(21) Illescas, B.; Martín, N.; Seoane, C. [60]Fullerene-based electron acceptors with tetracyano-*p*-quinodimethane (TCNQ) and dicyano-*p*-quinonediimine (DCNQI) derivatives. *Tetrahedron Lett.* **1997**, *38*, 2015−2018.
(22) Santos, J.; Pérez, E. M.; Illescas, B. M.; Martín, N. Linear and Hyperbranched Electron-Acceptor Supramolecular Oligomers. *Chem. - Asian J.* **2011**, *6*, 1848−1853.
(23) Urban, C.; Wang, Y.; Rodríguez-Fernández, J.; García, R.; Herranz, M. A.; Alcamí, M.; Martín, N.; Martín, F.; Gallego, J. M.; Miranda, R.; Otero, R. Charge transfer-assisted self-limited decyanation reaction of TCNQ-type electron acceptors on Cu(100). *Chem. Commun.* **2014**, *50*, 833−835.
(24) Chi, X.; Besnard, C.; Thorsmølle, V. K.; Butko, V. Y.; Taylor, A. J.; Siegrist, T.; Ramirez, A. P. Structure and Transport Properties of the Charge-Transfer Salt Coronene-TCNQ. *Chem. Mater.* **2004**, *16*, 5751−5755.
(25) Cadranel, A.; Strauss, V.; Margraf, J. T.; Winterfeld, K. A.; Vogl, C.; Đorđević, L.; Arcudi, F.; Hoelzel, H.; Jux, N.; Prato, M.; Guldi, D. M. Screening Supramolecular Interactions between Carbon Nanodots and Porphyrins. *J. Am. Chem. Soc.* **2018**, *140*, 904−907.
(26) Santos, J.; Illescas, B. M.; Martín, N.; Adrio, J.; Carretero, J. C.; Viruela, R.; Ortí, E.; Spänig, F.; Guldi, D. M. A Fully Conjugated TTF-π-TCAQ System: Synthesis, Structure, and Electronic Properties. *Chem. - Eur. J.* **2011**, *17*, 2957−2964.
(27) Kini, A. M.; Cowan, D. O.; Gerson, F.; Moeckel, R. New synthesis and properties of 11,11,12,12-tetracyano-9,10-anthraquinodimethane: an electron acceptor displaying a single-wave, two-electron reduction and a coproportionation pathway to the radical anion. *J. Am. Chem. Soc.* **1985**, *107*, 556−562.

https://dx.doi.org/10.1021/jacs.0c10132
J. Am. Chem. Soc. 2020, 142, 20324−20328